

# Theoretical Studies of Proton-Transfer Reactions of 2-Hydroxypyridine-(H<sub>2</sub>O)<sub>n</sub> (n = 0–2) in the Ground and Excited States

Quan-Song Li, Wei-Hai Fang,\* and Jian-Guo Yu

Department of Chemistry, Beijing Normal University, Beijing 100875, PR China

Received: December 3, 2004; In Final Form: March 12, 2005

The potential energy profiles for proton-transfer reactions of 2-hydroxypyridine and its complexes with water were determined by MP2, CASSCF and MR-CI calculations with the 6-31G\*\* basis set. The tautomerization reaction between 2-hydroxypyridine (2HP) and 2-pyridone (2PY) does not take place at room temperature because of a barrier of ~35 kcal/mol for the ground-state pathway. The water-catalyzed enol–keto tautomerization reactions in the ground state proceed easily through the concerted proton transfer, especially for the two-water complex. The S<sub>1</sub> tautomerization between the 2HP and 2PY monomers has a barrier of 18.4 kcal/mol, which is reduced to 5.6 kcal/mol for the one-water complex and 6.4 kcal/mol for the two-water complex. The results reported here predict that the photoinduced tautomerization reaction between the enol and keto forms involves a cyclic transition state having one or two water molecules as a bridge.

## 1. Introduction

Tautomerism phenomena have drawn the attention of biologists for many decades. For example, the tautomerism of purine and pyrimidine bases occurs naturally in nucleic acids, nucleotides, and enzymes, which may play a key role in mutagenesis.<sup>1</sup> The frequency of mispairing and thus mutagenesis in DNA is probably correlated with the amino–imino equilibrium.<sup>2,3</sup> 2-Hydroxypyridine exhibits two stable tautomeric forms: the enol form (2HP) and the keto form (2PY). The keto–enol tautomerization between 2HP and 2PY has been extensively investigated experimentally in various phases, in matrixes, and also theoretically as one of the simplest systems of intramolecular and intermolecular proton-transfer reactions.

Besides some early studies,<sup>4–8</sup> a number of experimental investigations have been devoted to spectroscopic features of 2HP, 2PY, and their complexes and the photoinduced enol–keto tautomerization in recent years.<sup>9–18</sup> It was found that in the gas phase the enol and keto forms are nearly equal in energy<sup>6,8</sup> but proton transfer proceeds with difficulty because of a large barrier for the ground-state pathway (16 000–20 000 cm<sup>-1</sup>).<sup>10,13</sup> Time-of-flight mass spectroscopy (TOFMS) and fluorescence excitation spectroscopy of the 2HP monomer have been studied under collision-free conditions in a supersonic jet expansion,<sup>10</sup> and the S<sub>0</sub>–S<sub>1</sub> band origin was observed at 36 136 cm<sup>-1</sup>. This band was identified as a  $\pi \rightarrow \pi^*$  transition. High-resolution rotationally resolved electronic spectra of 2HP at ~277 nm have been observed in the gas phase and fit using rigid-rotor Hamiltonians.<sup>17</sup> The derived values for the rotational constants are very similar to those for phenol. However, the electronic distributions in the N-heterocycle are significantly different from those of its hydrocarbon analogue.

The first absorption band system of 2PY in DMSO solution was observed in the range of 355–250 nm with the maximum at 305 nm for the monomer,<sup>7</sup> which corresponds to the  $\pi \rightarrow \pi^*$  transition. Two-color ionization spectra and dispersion fluorescence spectra of 2PY were studied by Nimlos and co-workers

in a supersonic jet.<sup>10</sup> The 2PY monomer was shown to be nonplanar in the ground state, giving rise to two origins in the excitation spectrum at 29 832 and 29 935 cm<sup>-1</sup>. The fluorescence excitation spectrum of 2PY–water in a supersonic free jet was recorded, and the two lowest-frequency bands at 29 832 and 29 927 cm<sup>-1</sup> were assigned as the electronic origins of two conformers of the 2PY monomers.<sup>11</sup> However, the 2PY monomer was shown to be planar and structurally identical in the S<sub>0</sub> state but differing in the degree of nonplanarity at the nitrogen atom in the S<sub>1</sub> state. Vibrational spectra of the key functional vibrations of 2PY, the H-bonded clusters with water, and the 2PY dimer in the gas phase have been investigated by using IR–UV and stimulated Raman–UV double-resonance methods combined with fluorescence detection.<sup>13,15</sup> The characteristic spectral changes upon cluster formation have been observed for the N–H and C=O stretching vibrations of the bare molecule. The 2PY monomer has two close-lying electronic states in the S<sub>1</sub> region, whose structures are slightly different with respect to the NH group.

Two-color resonance two-photon ionization and UV/UV–hole burning techniques<sup>14,16,18</sup> have been used to investigate the intermolecular vibrations of the supersonically cooled 2PY dimer and 2PY·2HP mixed dimer that are closely analogous to tautomeric H-bonded DNA base pairs. The three in-plane vibrations were observed in the S<sub>0</sub> and S<sub>1</sub> states, giving detailed information on the stretching and deformation force constants of the O–H···N and N–H···O=C hydrogen bonds. Structures of the 2PY–H<sub>2</sub>O and 2PY–(H<sub>2</sub>O)<sub>2</sub> complexes in their S<sub>0</sub> and S<sub>1</sub> electronic states have been determined from rotationally resolved S<sub>0</sub> → S<sub>1</sub> fluorescence excitation spectra.<sup>11</sup> The formation of the 2PY–(H<sub>2</sub>O)<sub>2</sub> complex was found to have a significant influence on the structure of the 2PY moiety and the heavy atoms are coplanar in the ground-state 2PY–(H<sub>2</sub>O)<sub>2</sub> complex. The band origins at ~35 468, 35 215, 30 473, and 30 728 cm<sup>-1</sup> were assigned to the S<sub>0</sub>–S<sub>1</sub> transitions of 2HP–H<sub>2</sub>O, 2HP–(H<sub>2</sub>O)<sub>2</sub>, 2PY–H<sub>2</sub>O, and 2PY–(H<sub>2</sub>O)<sub>2</sub>, respectively.<sup>10</sup>

Tautomerization reactions between 2HP and 2PY in the ground state have been the subject of numerous theoretical investigations.<sup>19–35</sup> Early in 1983, Hillier and co-workers<sup>19</sup>

\* Corresponding author. E-mail: fangwh@bnu.edu.cn. Tel: (+86)-10-5880-5382.

performed *ab initio* studies of the structures and relative stabilities of 2-, 3-, and 4-HP and the corresponding tautomers in the ground state. The water-catalyzed enol–keto tautomerization reactions in the ground state were further investigated<sup>20,21</sup> through a comparison of the three possible pathways: (i) direct proton transfer in the bare monomer, (ii) tautomeric interconversion within a self-associated dimer, and (iii) fully concerted proton transfer in the complex of 2HP–(H<sub>2</sub>O)<sub>2</sub>. In 1994, Gao and Shao<sup>24</sup> examined the role of electronic polarization effects in the tautomeric equilibrium of 2HP through Monte Carlo simulations using a combined quantum mechanical and molecular mechanical (QM/MM) potential. Their results indicated that different polarization in the hydroxy and oxo forms contributes significantly to the overall observed solvent effects in the tautomeric equilibrium, amounting to 14–68% of the total free energy of solvation in chloroform and in water.

In comparison with the tautomerization reactions in the ground state, the excited-state proton transfers in the 2HP monomer and 2HP–(H<sub>2</sub>O)<sub>*n*</sub> (*n* = 1, 2) complex have received less attention from theoretical chemists. As far as we know, there are only three reports that involve *ab initio* studies of excited-state proton-transfer reaction of the 2HP monomer.<sup>25,27,33</sup> Geometries of 2HP and 2PY were optimized at the HF level for the ground state and at the CIS and CASSCF levels for the excited states with C<sub>s</sub> symmetry constraints.<sup>25,27</sup> The potential energy profiles were determined as a function of the O–H or N–H distance by CASPT2 single-point calculations. It was found that there exists an intersection between the ground- and excited-state pathways of hydrogen atom transfer, from which Sobolewski and Adamowicz<sup>25,27</sup> came to the conclusion that the excited-state dissociation followed by the ground-state association of the hydrogen atom is the intrinsic feature of the photoinduced proton-transfer reaction and the photoinduced dissociation–association mechanism is responsible for the excited-state tautomerization observed in the system. However, the concerted reaction pathway has been determined for the excited-state tautomerization between 2HP and 2PY by CIS/6-31G\* calculations.<sup>33</sup> It is evident that there is only limited information from the *ab initio* study of the excited-state proton-transfer reactions of 2HP. In addition, photoinduced tautomerization reactions between 2HP–(H<sub>2</sub>O)<sub>*n*</sub> and 2PY–(H<sub>2</sub>O)<sub>*n*</sub> (*n* = 1, 2) were not investigated theoretically. In the present work, the ground- and excited-state proton-transfer processes of 2HP–(H<sub>2</sub>O)<sub>*n*</sub> (*n* = 0–2) have been investigated with advanced *ab initio* methods. We believe that the present study provides new insights into the mechanism of the photoinduced tautomerization between 2HP–(H<sub>2</sub>O)<sub>*n*</sub> and 2PY–(H<sub>2</sub>O)<sub>*n*</sub> (*n* = 0–2).

## 2. Computational Details

The stationary structures for the proton-transfer process of 2HP–(H<sub>2</sub>O)<sub>*n*</sub> (*n* = 0–2) in the ground and excited states have been optimized by means of the complete active space self-consistent-field (CASSCF) method, whereas the MP2 approach is used to optimize the structures in the ground state. For comparison, some structures in the ground state are also optimized at the B3LYP level. The 6-31G\*\* basis set, which has polarization functions on all atoms, is employed in the present investigation. Once convergence is reached, the harmonic frequencies are examined at this point to confirm that the geometry obtained is a true minimum or first-order saddle point. The optimization is terminated when the maximum force and its root mean square are less than 0.00045 and 0.0003 hartree/bohr, respectively. All optimizations were carried out using the Gaussian 98 package of programs.<sup>36</sup> Only tautomer-

ization reactions between 2HP–(H<sub>2</sub>O)<sub>*n*</sub> and 2PY–(H<sub>2</sub>O)<sub>*n*</sub> (*n* = 0–2) are investigated in the present work. The basis set superposition errors (BSSE) are partially canceled in the calculated relative energies of the 2HP and 2PY complexes. Therefore, the BSSE correction is not made in this study.

To describe the low-lying electronic states of 2HP, the three  $\pi$  and three  $\pi^*$  orbitals on the aromatic ring should be used as the active orbitals for the CASSCF calculations. Meanwhile, the nitrogen nonbonding orbital and the oxygen 2p<sub>z</sub> electrons are also included in the active space. This leads to the active space with 10 electrons in 8 orbitals, referred to as CAS(10,8) hereafter. In the calculation of the barrier heights and reaction energies, a factor of 0.89 is used to scale the zero-point vibrational energies and frequencies.<sup>37</sup> To refine the relative energies of the stationary structures, the single-point energy is calculated with the internally contracted MR-CI method that includes all single and double excitations relative to the CAS-(10,8) reference wave functions. The MOLPRO program package<sup>38</sup> was used to perform the MR-CI single-point energy calculations.

## 3. Results and Discussion

**A. Structures and Properties of Tautomers.** Let us start the discussion with an analysis of the structures of 2HP and 2PY monomers. The 2HP monomer has *trans* and *cis* conformers of the 2-OH group with respect to the ring N atom. Because the *cis* conformer is more stable, the *cis* monomer and its complexes are considered in the present work. 2HP and 2PY have planar structures in the ground state, which have been confirmed to be energy-minimum points by vibrational frequency calculations that give all real frequencies. The B3LYP, MP2, and CAS(10,8) optimized bond parameters and calculated energies for the 2HP and 2PY monomers in the ground and excited states are supplied as Supporting Information. Good agreement was found in the B3LYP and MP2 optimized bond lengths. The CAS(10,8)/6-31G\*\* optimized N1–C2, C2–O7, and O7–H8 bond lengths are about 0.02–0.04 Å shorter than the corresponding MP2 values. The other bond lengths in the ring are nearly unchanged from the MP2 to CAS(10,8) calculations. The selected MP2/6-31G\*\* and CAS(10,8) bond parameters are given in Figure 1a for 2HP and 2PY in the ground state. A comparison of the calculated rotational constants and dipole moments with the corresponding experimental values is made in Table 1 for 2HP and 2PY in the ground state, which reveals that the optimized 2HP and 2PY structures are reasonable.

From the viewpoint of valence bond theory, the interaction between the lone pair of the acceptor nitrogen atom and the O–H  $\sigma^*$  orbital is mainly responsible for the proton transfer from the oxygen to nitrogen atom. The N $\cdots$ H–O angle and N $\cdots$ H distance may play an important role in the proton-transfer reaction. In the 2HP monomer, the N1 $\cdots$ H8 distance is 2.238 Å, and the N1 $\cdots$ H8–O7 angle is about 81.2° at the MP2/6-31G\*\* level. In most cases, the hydrogen bond with linear N1 $\cdots$ H8–O7 structure is considered to be the strongest, and the weakest H-bond shows the largest deviation from linearity. The N1 $\cdots$ H8–O7 angle of 81.2° predicts that the intramolecular hydrogen (N $\cdots$ H–O) is very weak in the ground state of the 2HP monomer. The existence of the weak N $\cdots$ H–O hydrogen bond predicts that the tautomerization reaction has a considerably high barrier on the way from 2HP to 2PY and the reaction does not proceed easily in the ground state. An analogous situation was found for the proton transfer in the ground state of bare 7-HQ<sup>39</sup> or 8-HQ.<sup>40</sup>

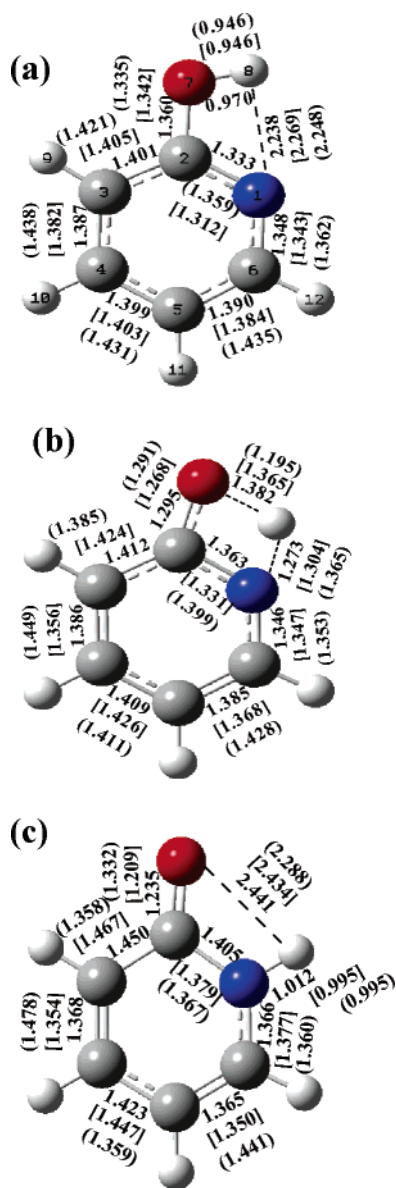


**Figure 1.** Schematic structures on the tautomerization pathways to the 2HP monomer, along with the MP2/6-31G\*\* bond lengths (in angstroms) for the ground state and CAS(10,8)/6-31G\*\* bond lengths (in angstroms) for both ground (in square brackets) and excited states (in parentheses), respectively. (a) 2HP, (b) 2HP-TS, and (c) 2PY.

The most striking change in structure is associated with electronic excitation. As in the ground state, 2HP in the excited state (2HP\*) has a planar equilibrium structure. Upon inspection of the geometries in Figure 1a, one can see that the ring N-C and C-C bond lengths are increased by 0.016–0.096 Å at the CAS(10,8)/6-31G\*\* level from the ground to excited states. The analysis of the natural orbital was performed on the basis of the CASSCF wave functions, which clearly shows that the optimized 2HP\* state is of  $^1\pi\pi^*$  character. The conjugation interaction in the ring is weakened by one-electron excitation from the  $\pi$  to the  $\pi^*$  orbital. As a result, the bond lengths in the ring are elongated, which is consistent with the CAS(10,8) optimized 2HP\* structure. Further evidence for this comes from the calculated rotational constants and dipole moments in Table 1, which are close to those inferred experimentally. On the basis of time-of-flight mass spectroscopy and fluorescence excitation spectrum studies,<sup>10</sup> Nimlos and co-workers suggested that the mixing of  $^1n\pi^*$  and  $^1\pi\pi^*$  states occurs in the first absorption band of 2HP. The  $^1n\pi^*$  electronic state was proposed to lie

**TABLE 1: Rotational Constants (MHz) and Dipole Moments (Debye) of  $2\text{HP}-(\text{H}_2\text{O})_n$  and  $2\text{PY}-(\text{H}_2\text{O})_n$  ( $n = 0-2$ ) in the Ground and Excited States**

parameter	A	B	C	$\mu_{\text{total}}$	
2HP	5825.0	2726.5	1876.2	1.39	expt <sup>a</sup>
	5872.1	2784.4	1888.8	1.51	calcd <sup>b</sup>
2HP*	5467.1	2780.5	1844.6		expt <sup>a</sup>
	5520.5	2741.1	1831.6	1.40	calcd <sup>b</sup>
2PY	5643.8	2793.5	1868.8	4.26	expt <sup>a</sup>
	5642.5	2824.5	1882.3	3.84	calcd <sup>b</sup>
2PY*					expt
	5583.6	2786.7	1861.2	1.68	calcd <sup>b</sup>
2HP-H <sub>2</sub> O					expt
	4036.1	1351.5	1015.2	2.96	calcd <sup>b</sup>
2HP*-H <sub>2</sub> O					expt
	3986.0	1317.9	993.0	2.89	calcd <sup>b</sup>
2PY-H <sub>2</sub> O					expt <sup>c</sup>
	3996.5	1394.1	1034.8		calcd <sup>b</sup>
	3973.7	1341.5	1005.3	3.06	calcd <sup>b</sup>
2PY*-H <sub>2</sub> O					expt <sup>c</sup>
	3933.4	1348.2	1006.4		calcd <sup>b</sup>
	3857.9	1314.1	983.2	2.30	calcd <sup>b</sup>
2HP-(H <sub>2</sub> O) <sub>2</sub>					expt
	2432.2	901.3	662.1	2.48	calcd <sup>b</sup>
2HP*-(H <sub>2</sub> O) <sub>2</sub>					expt
	2408.6	885.3	651.7	2.29	calcd <sup>b</sup>
2PY-(H <sub>2</sub> O) <sub>2</sub>					expt <sup>c</sup>
	2580.8	895.7	668.8		calcd <sup>b</sup>
	2548.3	856.2	644.8	2.22	calcd <sup>b</sup>
2PY*-(H <sub>2</sub> O) <sub>2</sub>					expt <sup>c</sup>
	2596.0	857.7	649.1		calcd <sup>b</sup>
	2649.6	804.1	621.1	1.38	calcd <sup>b</sup>

<sup>a</sup> Reference 17. <sup>b</sup> The cas (10,8)/6-31G\*\* calculated values. <sup>c</sup> Reference 11.

~2500  $\text{cm}^{-1}$  below the  $^1\pi\pi^*$  state. However, unsuccessful attempts were made to locate the origin of the  $n \rightarrow \pi^*$  transition of 2HP.<sup>10</sup> The  $^1n\pi^*$  electronic state of 2HP corresponds to one-electron excitation from the nitrogen or oxygen nonbonding orbital to the  $\pi^*$  orbital. The test CAS(10,8) optimizations and the MR-CI single-point energy calculations show that the  $^1n\pi^*$  state is much higher in energy than the  $^1\pi\pi^*$  state. The present calculations predict that the  $^1\pi\pi^*$  state is the first excited singlet state ( $S_1$ ) of the bare 2HP molecule. The  $S_0-S_1$  transition was assigned as the  $\pi \rightarrow \pi^*$  excitation for 2HP<sup>17</sup> because this transition was observed to be in-plane-polarized for 2HP. (An  $n \rightarrow \pi^*$  transition should be polarized perpendicular to the plane.)

The excited state of 2PY (2PY\*) was optimized at the CAS-(10,8) level, and the key bond parameters are given in Figure 1c. The calculated rotational constants and dipole moments are listed in Table 1, which are comparable to the experimentally inferred values. The natural orbital analysis on the CAS(10,8) wave functions shows that the first excited state ( $S_1$ ) of 2PY is mainly of  $^1\pi\pi^*$  character, which is consistent with the experimental assignment.<sup>10</sup> The heavy atoms are nearly coplanar in the 2PY\* structure, and the N1-H8 bond deviates from the plane by  $\sim \text{ThinSpace} \pm 27^\circ$ , giving rise to two minimum structures in the  $S_1$  state. Two intense peaks at 29 831 and 29 928  $\text{cm}^{-1}$  were observed in the TOF-MS spectra of the  $\pi \rightarrow \pi^*$  transition for the 2PY monomer, from which Nimlos and co-workers<sup>10</sup> suggested the presence of two ground-state conformations for 2PY. As pointed out before, the 2PY molecule has planar structure in the ground state, and there is only one conformation for the ground-state 2PY molecule. The present calculation predicts that the 2PY molecule has two minimum-energy structures in the  $S_1$  state, which are probably responsible for the two band origins observed experimentally. The fluorescence excitation spectrum of 2PY-water in a supersonic free jet was measured,<sup>11</sup> and the two lowest-frequency bands at 29 832 and 29 927  $\text{cm}^{-1}$  were identified as the electronic origins of two conformers of the 2PY monomer. However, the 2PY



molecule was inferred to be planar and structurally identical in the ground state but differing in the degree of nonplanarity of the nitrogen atom in the excited state.<sup>11</sup> From a fluorescence-detected IR spectroscopy study of 2PY,<sup>13</sup> Mikami and co-workers came to the conclusion that the two bands at 29 832 and 29 927  $\text{cm}^{-1}$  for 2PY originate from the same structure in the ground state. The  $S_1$ – $S_0$  spectrum was measured by using laser-induced fluorescence and population-labeling spectroscopy.<sup>15</sup> The results led to the conclusion that 2PY has two close-lying electronic states in the  $S_1$  region.

The equilibrium geometries of the 2HP complexes with one (2HP– $\text{H}_2\text{O}$ ) and two waters (2HP–( $\text{H}_2\text{O}$ )<sub>2</sub>) in the ground state are first optimized under the  $C_s$  symmetry constraint. The calculated frequencies showed that the optimized planar structures were not minimum points on the  $S_0$  surface. The nonplanar geometries were further optimized for 2HP– $\text{H}_2\text{O}$ , 2PY– $\text{H}_2\text{O}$ , 2HP–( $\text{H}_2\text{O}$ )<sub>2</sub>, and 2PY–( $\text{H}_2\text{O}$ )<sub>2</sub> at the B3LYP, MP2, and CAS-(10,8) levels with the 6-31G\*\* basis set and were confirmed to be minimum points by the frequency calculations. In the one-water complex, the O7–H8 bond length is about 0.01 Å longer than that in the 2HP monomer. The C2–O7 bond in the complex is shortened by about 0.01 Å, as compared with that in the 2HP monomer. However, the bond parameters in the ring are nearly unchanged from the monomer to the one-water complex. The O7–H8 bond is further increased, and the C2–O7 bond is further shortened from 2HP– $\text{H}_2\text{O}$  to 2HP–( $\text{H}_2\text{O}$ )<sub>2</sub>, as can be seen in Figures 1a, 2a, and 3a. The formation of the complex has a considerable influence on the –C–OH moiety of the 2HP monomer.

There are two intermolecular H-bonds of O7–H8···O13 and O13–H14···N1 in the 2HP– $\text{H}_2\text{O}$  complexes. The intermolecular H8···O13 and H14···N1 distances are respectively 1.950 and 2.167 Å in the ground state and become 1.925 and 2.159 Å in the first excited state of 2HP– $\text{H}_2\text{O}$  (2HP\*– $\text{H}_2\text{O}$ ). The intermolecular H-bond distances are significantly shortened from 2HP– $\text{H}_2\text{O}$  (2HP\*– $\text{H}_2\text{O}$ ) to 2HP–( $\text{H}_2\text{O}$ )<sub>2</sub> [2HP\*–( $\text{H}_2\text{O}$ )<sub>2</sub>]. The O7–H8···O13 and O13–H14···N1 angles are 161.7 and 138.5° in 2HP– $\text{H}_2\text{O}$  and 163.7 and 137.2° in 2HP\*– $\text{H}_2\text{O}$ , respectively. The O–H···O and O–H···N configurations are close to a linear arrangement in the ground and excited states of the two-water complexes. The optimized bond parameters clearly show that the intermolecular H-bonds in the complexes of 2HP–( $\text{H}_2\text{O}$ )<sub>*n*</sub> (*n* = 1, 2) are much stronger than the intramolecular H-bond in the 2HP monomer and the intermolecular H-bonds for the one- and two-water complexes are stronger in the  $S_1$  state than in the  $S_0$  state. All of these give us hints that the proton-transfer reactions take place more easily in the complexes than in the monomer, especially for the tautomerization reactions in the first excited state of the complexes. Further evidence for this comes from the calculated barriers on the tautomerization pathways, which will be discussed below.

The CAS(10,8)/6-31G\*\* optimized structures for the 2PY complexes with one and two  $\text{H}_2\text{O}$  molecules are schematically shown in Figures 2c and 3c, along with the selected bond parameters. The H14···O13 and H8···O7 distances in the 2PY– $\text{H}_2\text{O}$  complex are 2.104 and 2.048 Å, respectively, which are a little longer than the experimentally derived values of ~1.93 and 2.00 Å.<sup>11</sup> Upon electronic excitation to the  $S_1$  state, the H14···O13 and H8···O7 distances become 2.028 and 2.303 Å, respectively, at the CAS(10,8)/6-31G\*\* level. The H14···O13 and H8···O7 distances were experimentally estimated to be 2.06 and 2.05 Å, respectively.<sup>11</sup> The intermolecular H-bond distances (H17···O16, H15···O13, and H8···O7) in the two-water complex are significantly increased from the ground to excited state,

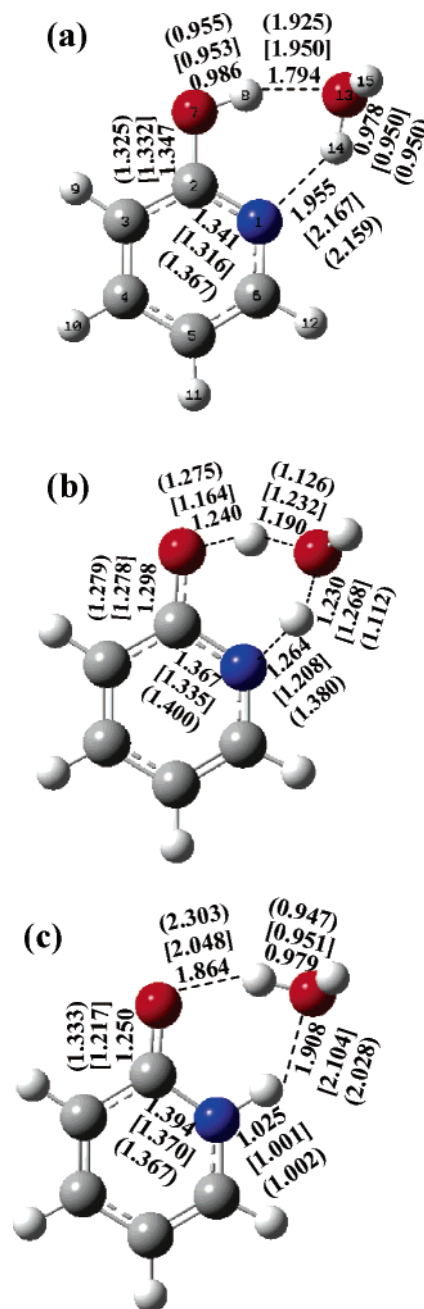


**Figure 2.** Schematic structures on the tautomerization pathways to the 2HP complex, along with the MP2/6-31G\*\* bond lengths (in angstroms) for the ground state and CAS(10,8)/6-31G\*\* bond lengths (in angstroms) for both ground (in square brackets) and excited states (in parentheses), respectively. (a) 2HP– $\text{H}_2\text{O}$ , (b) 2HP– $\text{H}_2\text{O}$ –TS, and (c) 2PY– $\text{H}_2\text{O}$ .

which can be seen from the intermolecular H-bond parameters in Figure 3c. The CAS(10,8)/6-31G\*\* optimized structures reveal that the intermolecular hydrogen bonds are stronger in the ground state than in the excited state for the 2PY– $\text{H}_2\text{O}$  and 2PY–( $\text{H}_2\text{O}$ )<sub>2</sub> complexes, which is different from the situation for the 2HP– $\text{H}_2\text{O}$  and 2HP–( $\text{H}_2\text{O}$ )<sub>2</sub> complexes where the H-bond strengths increase from the  $S_0$  to  $S_1$  state. Experimentally, it has been found that the complexation of 2PY with water produces a blue shift in the electronic origins of both 2PY– $\text{H}_2\text{O}$  and 2PY–( $\text{H}_2\text{O}$ )<sub>2</sub> relative to the monomer origins,<sup>10,11</sup> which is in agreement with the weaker H-bond formed between the  $S_1$  2PY and water than between the  $S_0$  2PY and water. In addition, the band origin of 36 136  $\text{cm}^{-1}$  for the 2HP monomer is red shifted to 35 468 for 2HP– $\text{H}_2\text{O}$  and to 35 215  $\text{cm}^{-1}$  for

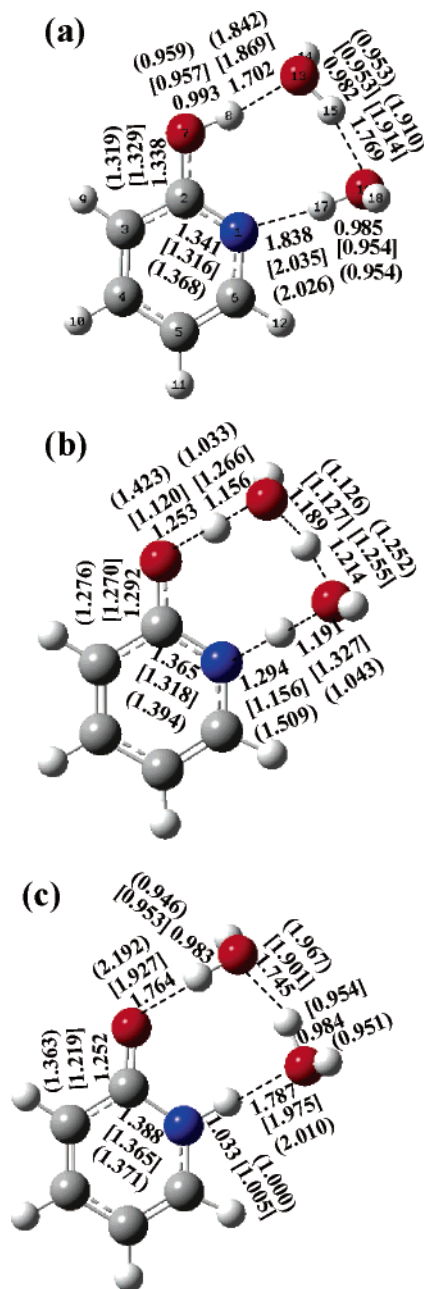


**Figure 3.** Schematic structures on the tautomerization pathways to the 2HP complex, along with the MP2/6-31G\*\* bond lengths (in angstroms) for the ground state and CAS(10,8)/6-31G\*\* bond lengths (in angstroms) for both ground (in square brackets) and excited states (in parentheses), respectively. (a)  $2\text{HP}-(\text{H}_2\text{O})_2$ , (b)  $2\text{HP}-(\text{H}_2\text{O})_2\text{-TS}$ , and (c)  $2\text{PY}-(\text{H}_2\text{O})_2$ .

$2\text{HP}-(\text{H}_2\text{O})_2$ .<sup>10,13</sup> The red shift of the band origin upon complexation shows that the interaction between 2HP and water is stronger in  $S_1$  than in  $S_0$ .

As pointed out before, the bond parameters in the ring are almost unchanged from the monomer to the complexes. However, the formation of a complex has a considerable influence on the O–H or N–H structure of the monomer. The CAS(10,8)/6-31G\*\* calculated O–H, C=O, and N–H stretching vibrational frequencies scaled by a factor of 0.89 are listed in Table 2 for the monomers and complexes, together with experimental values where available. The N–H and C=O stretching frequencies are respectively predicted to be 3453 and 1733  $\text{cm}^{-1}$  in 2PY. Upon formation of the  $2\text{PY}-(\text{H}_2\text{O})_2$  complex, the N–H and C=O stretching frequencies are reduced to 3368

**TABLE 2: N–H, C=O, and O–H Stretching Vibrational Frequencies ( $\text{cm}^{-1}$ ) of  $2\text{PY}-(\text{H}_2\text{O})_n$  and  $2\text{HP}-(\text{H}_2\text{O})_n$  ( $n = 0-2$ ) in the Ground and Excited States**

modes	2PY	2PY*	2PY– H <sub>2</sub> O	2PY*– H <sub>2</sub> O	2PY– (H <sub>2</sub> O) <sub>2</sub>	2PY*– (H <sub>2</sub> O) <sub>2</sub>	
N–H	3453	3431	3368	3389	3304	3302	calcd <sup>a</sup>
	3448	3410	3329	3287			expt <sup>b</sup>
C=O	1733	1215	1717	1079	1712	1068	calcd <sup>a</sup>
	1721		1707				expt <sup>b</sup>
	2HP	2HP*	2HP– H <sub>2</sub> O	2HP*– H <sub>2</sub> O	2HP– (H <sub>2</sub> O) <sub>2</sub>	2HP*– (H <sub>2</sub> O) <sub>2</sub>	
O–H	3703	3695	3552	3527	3485	3448	calcd <sup>a</sup>

<sup>a</sup> The cas (10,8)/6-31G\*\* calculated values scaled by a factor of 0.89 (ref 37). <sup>b</sup> References 13 and 15.

and 1717  $\text{cm}^{-1}$ , respectively. The calculated frequencies are very close to corresponding experimental values<sup>13</sup> of 3448 and 1721  $\text{cm}^{-1}$  in 2PY and 3329 and 1707  $\text{cm}^{-1}$  in  $2\text{PY}-(\text{H}_2\text{O})_2$ . An electronic excitation has a small influence on the N–H stretching vibration, but the C=O stretching frequency is significantly decreased from  $S_0$  to  $S_1$ . The computed N–H stretching frequency is 3431  $\text{cm}^{-1}$  in  $2\text{PY}^*$  and 3389  $\text{cm}^{-1}$  in  $2\text{PY}^*-(\text{H}_2\text{O})_2$ . The N–H stretching frequencies of  $2\text{PY}^*$  and  $2\text{PY}^*-(\text{H}_2\text{O})_2$  were experimentally estimated to be 3410 and 3287  $\text{cm}^{-1}$ , respectively.<sup>15</sup>

**B. Relative Energies of Isomers.** The energy difference between 2HP and 2PY is calculated to be 0.1, 2.4, and 0.1 kcal/mol at the B3LYP/6-31G\*\*, MP2/6-31G\*\*, and CAS(10,8)/6-31G\*\* levels, respectively, with the 2HP isomer being more stable. Previous experiments<sup>6,8,10</sup> have proven that under isolated molecule conditions (e.g., supersonic jet, gas phase, inert matrixes) the free-energy difference between 2HP and 2PY is about 0.02–0.04 eV in favor of the former. The energy difference between 2HP and 2PY is slightly influenced by the formation of the complex with water, as shown in the lower parts of Figure 4a–c. Unlike the ground state where  $2\text{HP}-(\text{H}_2\text{O})_n$  is more stable than  $2\text{PY}-(\text{H}_2\text{O})_n$  ( $n = 0, 1, 2$ ), in the excited state  $2\text{PY}^*-(\text{H}_2\text{O})_n$  is lower in energy than  $2\text{HP}^*-(\text{H}_2\text{O})_n$  ( $n = 0, 1, 2$ ). The energy difference between  $2\text{PY}^*$  and  $2\text{HP}^*$  is predicted to be 17.2 kcal/mol by the MR-CI calculations. The tautomerization reaction from  $2\text{HP}^*$  to  $2\text{PY}^*$  is experimentally inferred to be exothermic by  $\sim 6500 \text{ cm}^{-1}$  (18.6 kcal/mol),<sup>10</sup> which is very close to the MR-CI calculated value. The MR-CI calculations predict that the tautomerization reaction from  $2\text{HP}^*-(\text{H}_2\text{O})_n$  to  $2\text{PY}^*-(\text{H}_2\text{O})_n$  ( $n = 1, 2$ ) is exothermic by 16.0 kcal/mol for the one-water complex and 19.6 kcal/mol for the two-water complex.

The adiabatic transition energy (0–0 energy gap) from the ground state to the first excited singlet state was calculated by CAS(10,8) and MRCI methods. The 0–0 energies for 2HP,  $2\text{HP}-(\text{H}_2\text{O})_2$ , and  $2\text{HP}-(\text{H}_2\text{O})_2$  were predicted to be 109.3, 108.8, and 108.2 kcal/mol, respectively, at the CAS(10,8)/6-31G\*\* level with the zero-point energy correction. They become 111.1, 109.0, and 109.9 kcal/mol, respectively, by MR-CI single-point calculations. In a recent experimental study of 2HP by high-resolution electronic spectra,<sup>17</sup> the  $S_0-S_1$  band origin of bare 2HP was observed at 36 118.7  $\text{cm}^{-1}$  (103.3 kcal/mol), which is close to the value of 36 136  $\text{cm}^{-1}$  reported by Nimlos et al.<sup>10</sup> Additionally, the band origins at 35 468 (101.4 kcal/mol) and 35 215  $\text{cm}^{-1}$  (100.7 kcal/mol) were assigned to the  $S_0-S_1$  transitions of  $2\text{HP}-(\text{H}_2\text{O})_2$  and  $2\text{HP}-(\text{H}_2\text{O})_2$ , respectively.<sup>10</sup>

The 0–0 energies for  $2\text{PY}$ ,  $2\text{PY}-(\text{H}_2\text{O})_2$ , and  $2\text{PY}-(\text{H}_2\text{O})_2$  were predicted to be 86.9, 86.1, and 87.8 kcal/mol by the CAS(10,8)/6-31G\*\* calculations and 94.2, 96.0, and 94.0 kcal/mol

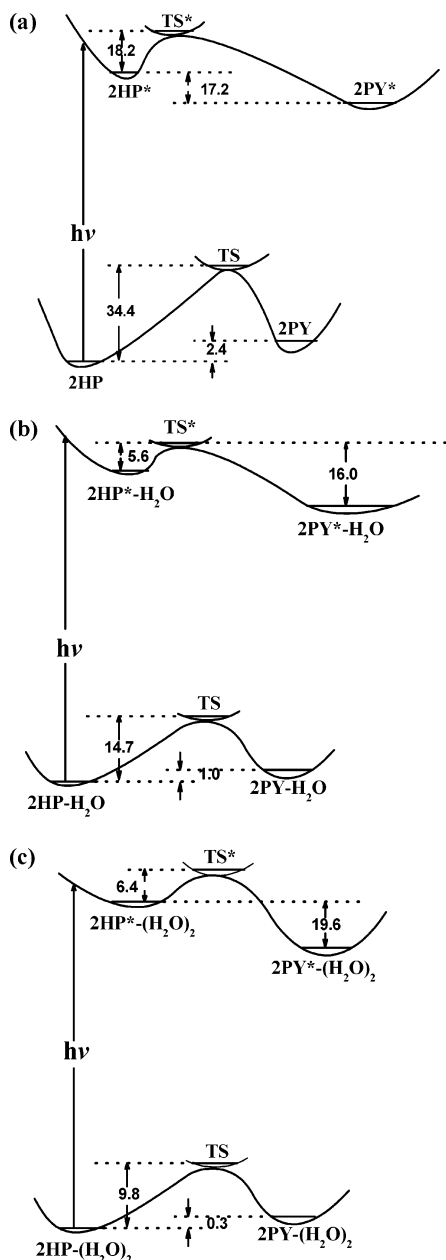


**Figure 4.** Schematic potential energy surfaces for tautomerization reactions of  $2\text{HP}-(\text{H}_2\text{O})_n$ , along with the MP2/6-31G\*\* relative energies (in kcal/mol) for the ground state and MR-CI relative energies (in kcal/mol) for the excited state, respectively. (a)  $n = 0$ , (b)  $n = 1$ , and (c)  $n = 2$ .

by the MR-CI single point calculations with the corresponding zero-point energy correction, respectively. Nimlos et al.<sup>10</sup> reported that the  $\pi \rightarrow \pi^*$  transition of 2PY has two origins at 29 832 (85.3) and 29 935  $\text{cm}^{-1}$  (85.6 kcal/mol). The band origins at 30 473 (87.1) and 30 728  $\text{cm}^{-1}$  (87.9 kcal/mol) were assigned to the  $S_0$ – $S_1$  transitions of  $2\text{PY}-\text{H}_2\text{O}$  and  $2\text{PY}-(\text{H}_2\text{O})_2$ , respectively.<sup>10</sup> In comparison with the experimental values, the MR-CI calculations overestimate the adiabatic excitation energy by a few kcal/mol.

**C. Tautomerization Reactions** A transition state, referred to as 2HP–TS hereafter, was found for the tautomerization reaction from 2HP to 2PY in the ground state. Similar to 2HP and 2PY, the 2HP–TS transition state has a planar structure, which is confirmed to be the first-order saddle point on the tautomerization pathway. The selected MP2/6-31G\*\* and CAS-(10,8)/6-31G\*\* bond distances are given in Figure 1b. In the

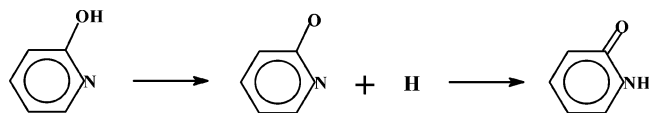
2HP–TS structure, the H8–O7 distance is 1.382 Å and the N1–H8 separation is 1.273 Å at the MP2/6-31G\*\* level. This reveals that the O–H bond is nearly broken and the N–H bond is almost formed in 2HP–TS. With respect to the 2HP minimum, the tautomerization reaction in the ground state has a barrier of 34.4 kcal/mol at the MP2/6-31G\*\* level. The activation energy for the ground-state tautomerization from 2HP to 2PY was calculated to be 42.8 kcal/mol at the CI/RHF/3-21G level.<sup>20</sup> The B3LYP/TZ2P calculations by Barone and Adamo<sup>41</sup> provided a barrier of 35–38 kcal/mol for the tautomerization between 2HP and 2PY in the ground state, which is close to the value reported here. In the gas phase, proton transfer from 2HP to 2PY was experimentally estimated to have a barrier of  $\sim 45$  kcal/mol ( $\sim 16\,000\text{ cm}^{-1}$ ).<sup>13</sup> A barrier of 35–45 kcal/mol predicts that the isomerization reaction from 2HP to 2PY in the ground state does not proceed at room temperature.

In the complex of  $2\text{HP}-\text{H}_2\text{O}$ , the proton-transfer reactions occur with  $\text{H}_2\text{O}$  as a bridge. Figure 2b shows the optimized geometries of the transition state ( $2\text{HP}-\text{H}_2\text{O}-\text{TS}$ ) along with the MP2/6-31G\*\* parameters. From the structure of  $2\text{HP}-\text{H}_2\text{O}-\text{TS}$  in Figure 2b, we can easily see that the H8 transfer from O7 to O13 is accompanied by the H14 transfer from O13 to N1. A similar situation can be seen in Figure 3b for  $2\text{HP}-(\text{H}_2\text{O})_2-\text{TS}$ . Actually, the tautomerization reaction between  $2\text{HP}-\text{H}_2\text{O}$  and  $2\text{PY}-\text{H}_2\text{O}$  or between  $2\text{HP}-(\text{H}_2\text{O})_2$  and  $2\text{PY}-(\text{H}_2\text{O})_2$  is a concerted process in the ground state. The barrier height was predicted to be 14.7 and 9.8 kcal/mol at the MP2/6-31G\*\* level, respectively, which is much lower than 34.4 kcal/mol for the tautomerization reaction between the 2HP and 2PY monomers. The  $2\text{HP}-(\text{H}_2\text{O})_2$ ,  $2\text{HP}-(\text{H}_2\text{O})_2-\text{TS}$ , and  $2\text{PY}-(\text{H}_2\text{O})_2$  structures were optimized at the HF/3-21G level, which is followed by the CI single-point energy calculations.<sup>20</sup> The barrier height was predicted to be 10.2 kcal/mol for the tautomerization between  $2\text{HP}-(\text{H}_2\text{O})_2$  and  $2\text{PY}-(\text{H}_2\text{O})_2$ . While this manuscript was in revision, Yamabe et al.<sup>42</sup> reported a theoretical study of the tautomerization paths of  $2\text{HP}-(\text{H}_2\text{O})_n$  to  $2\text{PY}-(\text{H}_2\text{O})_n$  ( $n = 0$ –3) in the ground state. The 2HP molecule was found to be isomerized most readily and concertedly to the 2PY molecule via proton relays with two water molecules. The barrier height was predicted to be 8.4 kcal/mol at the B3LYP/6-31G\* level.

Here we pay attention to the tautomerization reactions occurring along the excited-state pathways. A transition state, labeled 2HP\*–TS, is optimized at the CAS(10,8) level of theory for the tautomerization between 2HP and 2PY in the  $S_1$  electronic state. The resulting structure is schematically shown in Figure 1b along with the key CAS(10,8)/6-31G\*\* bond parameters. The H8–O7 distance is 1.195 Å, whereas the N1–H8 separation is 1.365 Å in 2HP\*–TS. It is clear that the 2HP\*–TS structure is more reactant-like because the reaction is exothermic along the  $S_1$  pathway. The barrier to the tautomerization along the  $S_1$  pathway was predicted to be 18.2 kcal/mol by the MR-CI calculations. However, relative to the  $S_0$  minimum, the 2HP\*–TS transition state has an energy of 129.3 kcal/mol. The  $S_1$  tautomerization reaction is not accessible in energy upon photoexcitation at  $\sim 277\text{ nm}$ , which corresponds to the transition energy of  $\sim 103$  kcal/mol. Therefore, the isomerization reaction from 2HP\* to 2PY\* does not proceed under this condition. The dispersed emission spectrum of the 2HP molecule was observed upon excitation of this molecule at  $\sim 277\text{ nm}$ , and the emission was found to originate from the excited state of the 2HP molecule but not from the 2PY excited state.<sup>10</sup> This suggests that the excited-state intramolecular proton transfer does not occur in the bare molecule.



## SCHEME 1



As discussed before, the CAS(10,8) calculated adiabatic excitation energies are close to the experimentally observed  $S_0$ – $S_1$  band origins. However, the barrier to  $S_1$  tautomerization was remarkably overestimated by the CAS(10,8) computations. The orbital energies of the  $\sigma$  orbitals are much lower than those of the conjugation  $\pi$  orbitals and oxygen and nitrogen  $n$  orbitals for the equilibrium geometries of 2HP and 2PY in the  $S_0$  and  $S_1$  states. The near-degenerate orbitals are included in the (10,8) active space for the  $S_0$  and  $S_1$  equilibrium geometries. This is one of the main reasons that the CAS(10,8) calculations can provide a good description of the adiabatic excitation energies for the monomers and their complexes. The tautomerization processes involve the formation and breakage of the O–H and N–H bonds; the O–H and N–H  $\sigma$  and  $\sigma^*$  orbitals are included in the active space for the CAS(10,8) optimizations of the  $S_1$  transition states. Some of the  $\pi$  electrons were treated as filled closed-shell orbitals with no recovery of correlation energy. Therefore, the CAS(10,8) calculations overestimate the barrier to the  $S_1$  tautomerization, which is significantly improved by the MR-CI calculations.

As with the complex in the ground state, the excited-state proton transfer is also a concerted process, which can be seen from the structural parameters of 2HP\*–H<sub>2</sub>O–TS in Figure 2b and 2HP\*–(H<sub>2</sub>O)<sub>2</sub>–TS in Figure 3b. The potential energy profiles for the excited-state proton-transfer reactions are shown in the upper parts of Figure 4b and 4c. The barriers to the  $S_1$  tautomerization reactions are 5.6 kcal/mol for the one-water complex and 6.4 kcal/mol for the two-water complex at the MR-CI level of theory. The calculated barrier heights predict that the excited-state proton transfer can take place in the complexes. Some vibrational levels of van der Waals (vdW) modes were observed in TOF-MS spectra of the disolvated water cluster of 2HP but were not observed for the monosolvated cluster. This shows that the H-bond between H<sub>2</sub>O and 2HP is stronger in the disolvated cluster than in the monosolvated cluster.<sup>10</sup> The vdW vibrational activity in the disolvated water cluster is suggestive of excited-state proton transfer.

Sobolewski and Adamowicz<sup>25,27</sup> suggested the photoinduced dissociation–association (PIDA) mechanism for the excited-state tautomerization between 2HP and 2PY, which is described in Scheme 1.

The first step in the PIDA mechanism involves O–H bond dissociation, which is followed by N–H bond formation in the second step. Sobolewski and Adamowicz<sup>27</sup> noticed that a rather large barrier exists for the excited-state dissociation pathway and speculated that excitation to higher electronic states may provide a driving force for the dissociation of the hydrogen atom. The PIDA mechanism proposed by Sobolewski and Adamowicz<sup>25,27</sup> is not supported by the present calculations, which give evidence that the tautomerization reactions proceed via a concerted mechanism. Barone and Adamo<sup>33</sup> performed ab initio calculations on the isomerization reactions and pointed out that the reactions are concerted processes. On the basis of the spectral data, Nimlos et al.<sup>10</sup> believed that excited-state tautomerization is likely in the disolvated water cluster of 2HP, which is consistent with the conclusions from the present study.

## 4. Summary

In this paper, the MP2, CASSCF, and MR-CI methods were used to investigate the proton-transfer reactions of the 2HP monomer and its one- and two-water complexes. The  $S_0$  and  $S_1$  equilibrium geometries and the potential energy profiles of the reactions were determined by the MP2, CASSCF, and MR-CI calculations with the 6-31G\*\* basis set. The two tautomers of 2HP and 2PY are planar in the ground state, and the tautomerization between 2HP and 2PY does not take place in the ground state because of a barrier of 34.4 kcal/mol for the pathway. One or two water molecules act as a bridge, which makes proton transfer easy in the complexes, especially in the two-water complex. The barrier height for the  $S_0$  pathways was reduced to 14.7 and 9.8 kcal/mol for 2HP–H<sub>2</sub>O and 2HP–(H<sub>2</sub>O)<sub>2</sub>, respectively. The calculated barriers show that the water-catalyzed enol–keto tautomerization reactions in the ground state proceed easily through the concerted proton-transfer mechanism.

Photoexcitation at  $\sim 277$  nm leads to the monomer and complexes in the  $S_1$  state, which corresponds to a  $\pi \rightarrow \pi^*$  transition mainly localized in the ring. The intramolecular proton-transfer reaction from 2HP\* to 2PY\* does not occur at this excitation wavelength. The barrier to the  $S_1$  proton transfer was reduced to 5.6 kcal/mol for 2HP\*–H<sub>2</sub>O and 6.4 kcal/mol for 2HP\*–(H<sub>2</sub>O)<sub>2</sub>. The results reported here predict that the photoinduced tautomerization reaction can occur in the one- or two-water complexes, which involves a concerted proton transfer through a cyclic transition state.

**Acknowledgment.** This work was supported by grants from the National Natural Science Foundation of China (grant nos. 20472011 and 20233020) and from the Major State Basic Research Development Programs (grant nos. 2004CB719903 and 2002CB613406).

**Supporting Information Available:** Structures, energies, and vibrational frequencies for all stationary points reported in the present work. This material is available free of charge via the Internet at <http://pubs.acs.org>.

## References and Notes

- (1) Pullman, B.; Oullman, A. *Adv. Heterocycl. Chem.* **1971**, *13*, 77.
- (2) Cantor, C. R.; Schimmel, P. R. *Biophysical Chemistry I*; Freeman: San Francisco, 1980; p 1.
- (3) Arnaut, L. G.; Formosinho, S. J. *J. Photochem. Photobiol., A* **1993**, *75*, 1.
- (4) Mason, S. F. *J. Chem. Soc.* **1958**, 674.
- (5) Elguero, J.; Marzin, C.; Katritzky, A. R.; Linda, P. *The Tautomerism of Heterocycles*; Academic: New York, 1976.
- (6) Beak, P. *Acc. Chem. Res.* **1977**, *10*, 186.
- (7) Fujimoto, A.; Inuzuka, K.; Shiba, R. *Bull. Chem. Soc. Jpn.* **1981**, *54*, 2802.
- (8) Krebs, C.; Forster, W.; Weiss, C.; Hofmann, H. J. *J. Prakt. Chem.* **1982**, *324*, 369.
- (9) Bensaude, O.; Dreyfus, M.; Dodin, G.; Dubois, J. E. *J. Am. Chem. Soc.* **1987**, *99*, 4438.
- (10) Nimlos, M. R.; Kelley, D. F.; Bernstein, E. R. *J. Phys. Chem.* **1989**, *93*, 643 and references therein.
- (11) Held, A.; Pratt, D. W. *J. Am. Chem. Soc.* **1993**, *115*, 9708.
- (12) Ozeki, H.; Cochet, M. C. R.; Okuyama, K.; Takahashi, M.; Kimura, K. *J. Phys. Chem.* **1995**, *99*, 8608.
- (13) Matsuda, Y.; Ebata, T.; Mikami, N. *J. Chem. Phys.* **1999**, *110*, 8397 and references therein.
- (14) Muller, A.; Talbot, F.; Leutwyler, S. *J. Chem. Phys.* **2000**, *112*, 3717.
- (15) Matsuda, Y.; Ebata, T.; Mikami, N. *J. Chem. Phys.* **2000**, *113*, 573.
- (16) Muller, A.; Talbot, F.; Leutwyler, S. *J. Chem. Phys.* **2001**, *115*, 5192 and references therein.
- (17) Borst, D. R.; Roscioli, J. R.; Pratt, D. W. *J. Phys. Chem. A* **2002**, *106*, 4022, and references therein.

- (18) Muller, A.; Talbot, F.; Leutwyler, S. *J. Am. Chem. Soc.* **2002**, *124*, 14486 and references therein.
- (19) Scanlan, M. J.; Hillier, I. H.; MacDowell, A. A. *J. Am. Chem. Soc.* **1983**, *105*, 3568.
- (20) Field, M. J.; Hillier, I. H.; Guest, M. F. *J. Chem. Soc., Chem. Commun.* **1984**, 1310.
- (21) Field, M. J.; Hillier, I. H. *J. Chem. Soc., Perkin Trans.* **1987**, 617.
- (22) Person, W. B.; Del Bene, J. E.; Szajda, W.; Szczepaniak, K.; Szczesniak, M. *J. Phys. Chem.* **1991**, *95*, 2770.
- (23) Wong, M. W.; Wiberg, K. B.; Frisch, M. J. *J. Am. Chem. Soc.* **1992**, *114*, 1645.
- (24) Gao, J.; Shao, L. *J. Phys. Chem.* **1994**, *98*, 13772.
- (25) Sobolewski, A. L. *Chem. Phys. Lett.* **1993**, *211*, 293.
- (26) Buyl, F.; Smets, J.; Maes, G.; Adamowicz, L. *J. Phys. Chem.* **1995**, *99*, 14967.
- (27) Sobolewski, A. L.; Adamowicz, L. *J. Phys. Chem.* **1996**, *100*, 3933.
- (28) Wang, J.; Boyd, R. J. *J. Phys. Chem.* **1996**, *100*, 16141.
- (29) Chou, P.-T.; Wei, C.-Y. *J. Phys. Chem. B* **1997**, *101*, 9119.
- (30) Kaminski, G. A.; Jorgensen, W. L. *J. Phys. Chem. B* **1998**, *102*, 1787.
- (31) Alkorta, I.; Elguero, J. *J. Org. Chem.* **2002**, *67*, 1515.
- (32) Nowak, M. J.; Lapinski, L.; Fulara, J.; Les, A.; Adamowicz, L. *J. Phys. Chem.* **1992**, *96*, 1562. Dkhissi, A.; Houben, L.; Smets, J.; Adamowicz, L.; Maes, G. *J. Phys. Chem. A* **2000**, *104*, 9785.
- (33) Barone, V.; Adamo, C. *Chem. Phys. Lett.* **1994**, *226*, 399.
- (34) Sato, H.; Hirata, F.; Sakaki, S. *J. Phys. Chem. A* **2004**, *108*, 2097.
- (35) Smedarchina, Z.; Siebrand, W.; Fernández-Ramos, A.; Martínez-Núñez, E. *Chem. Phys. Lett.* **2004**, *386*, 396.
- (36) Frisch, M. J.; Trucks, G. W.; Schlegel, H. B.; Scuseria, G. E.; Robb, M. A.; Cheeseman, J. R.; Zakrzewski, V. G.; Montgomery, J. A., Jr.; Stratmann, R. E.; Burant, J. C.; Dapprich, S.; Millam, J. M.; Daniels, A. D.; Kudin, K. N.; Strain, M. C.; Farkas, O.; Tomasi, J.; Barone, V.; Cossi, M.; Cammi, R.; Mennucci, B.; Pomelli, C.; Adamo, C.; Clifford, S.; Ochterski, J.; Petersson, G. A.; Ayala, P. Y.; Cui, Q.; Morokuma, K.; Malick, D. K.; Rabuck, A. D.; Raghavachari, K.; Foresman, J. B.; Cioslowski, J.; Ortiz, J. V.; Baboul, A. G.; Stefanov, B. B.; Liu, G.; Liashenko, A.; Piskorz, P.; Komaromi, I.; Gomperts, R.; Martin, R. L.; Fox, D. J.; Keith, T.; Al-Laham, M. A.; Peng, C. Y.; Nanayakkara, A.; Gonzalez, C.; Challacombe, M.; Gill, P. M. W.; Johnson, B.; Chen, W.; Wong, M. W.; Andres, J. L.; Gonzalez, C.; Head-Gordon, M.; Replogle, S.; Pople, J. A. *Gaussian 98*, revision A.7; Gaussian, Inc.: Pittsburgh, PA, 1998.
- (37) Scott, A. P.; Radom, L. *J. Phys. Chem. A* **1996**, *100*, 16502.
- (38) MOLPRO is a package of ab initio programs written by Werner, H.-J. and Knowles, P. J. with contributions from Almlof, J.; Amos, R. D.; Cooper, D. L.; Deegan, M. J. O.; Dobbyn, A. J.; Eclert, E.; Elbert, S. T.; Hampel, C.; Lindh, R.; Lloyd, A. W.; Meyer, W.; Nicklass, A.; Peterson, K.; Pitzer, R.; Stone, A. J.; Taylor, P. R.; Mura, M. E.; Pulay, P.; Schutz, M.; Stoll, H.; Thorsteinsson, T.
- (39) Fang, W. H. *J. Am. Chem. Soc.* **1998**, *120*, 7568.
- (40) Li, Q. S.; Fang, W. H. *Chem. Phys. Lett.* **2003**, *367*, 637.
- (41) Barone, V.; Adamo, C. *J. Phys. Chem.* **1995**, *99*, 150 62.
- (42) Tsuchida, N.; Yamabe, S. *J. Phys. Chem. A* **2005**, *109*, 1974